Determining Rainfall Intensity and Type from GOES Imagery in the Midlatitudes

A. A. TSONIS

Department of Geological and Geophysical Sciences, University of Wisconsin-Milwaukee, Milwaukee, Wisconsin 53201

Although a useful estimate of the areal extent of precipitation from visible and infrared satellite data can be made, the extraction of rainfall rates is still a problem. Earlier work by the author suggested that little, if any, correlation exists between rainfall rate and brightness or cloud top temperature individually. The results of this work indicate that by employing pattern matching techniques it may be possible to objectively define a satellite delineated rain area in terms of light–moderate and moderate–heavy. Further, convective and nonconvective precipitation areas can be separated.

Introduction

The estimation of rain from the Geostationary Orbiting Environmental Satellite (GOES) visible and/or infrared imagery has received during the past fifteen years much attention. A comprehensive review of rain area estimation from satellites up to 1981 was gathered by Barrett and Martin (1981). In general, the majority of the techniques can be divided in mono-spectral methods, [Scofield and Oliver (1977), Griffith et al. (1978) and Stout et al. (1979), for example] and bi-spectral methods [Lovejoy and Austin (1979) and Tsonis and Isaac (1985), for example]. Although the rain area delineation from the GOES images is progressively improving, attempts to relate the cloud brightness (visible information) and/or the cloud top temperature (infrared information) to the *rainfall rate* have not been very successful. Part of the problem lies in the fact that high cloud brightness values or low cloud temperatures can in fact result from nonraining clouds. Recently, Wu et al. (1985) presented a rather sophisticated method for classification of the satellite derived rain area into light and heavy rain areas. Their approach makes use of the textural and spectral properties of the visible and infrared fields mainly over tropical storms. It seems that textural properties will not serve as good discriminators for rainrates in the midlatitudes where less convection is generally available. Tsonis (1984) observed that, in some nonconvective cases, texture by itself was not able to discriminate between rain and no rain. This study presents some preliminary results of a different approach which could be used to delineate rainrate information from the GOES images in the midlatitudes, and to differentiate between convective and nonconvective precipitation.

Data

The satellite data used in this work are GOES east visible (0.54–0.70 μm wavelength) and thermal infrared (10.5–12.6 μm wavelength) images. The temporal resolution of the satellite data is 30 minutes and the spatial visible resolution is 4×4 km. The resolution of the infrared

52 Vanderbilt Ave., New York, NY 10017 0034-4257/87/$3.50

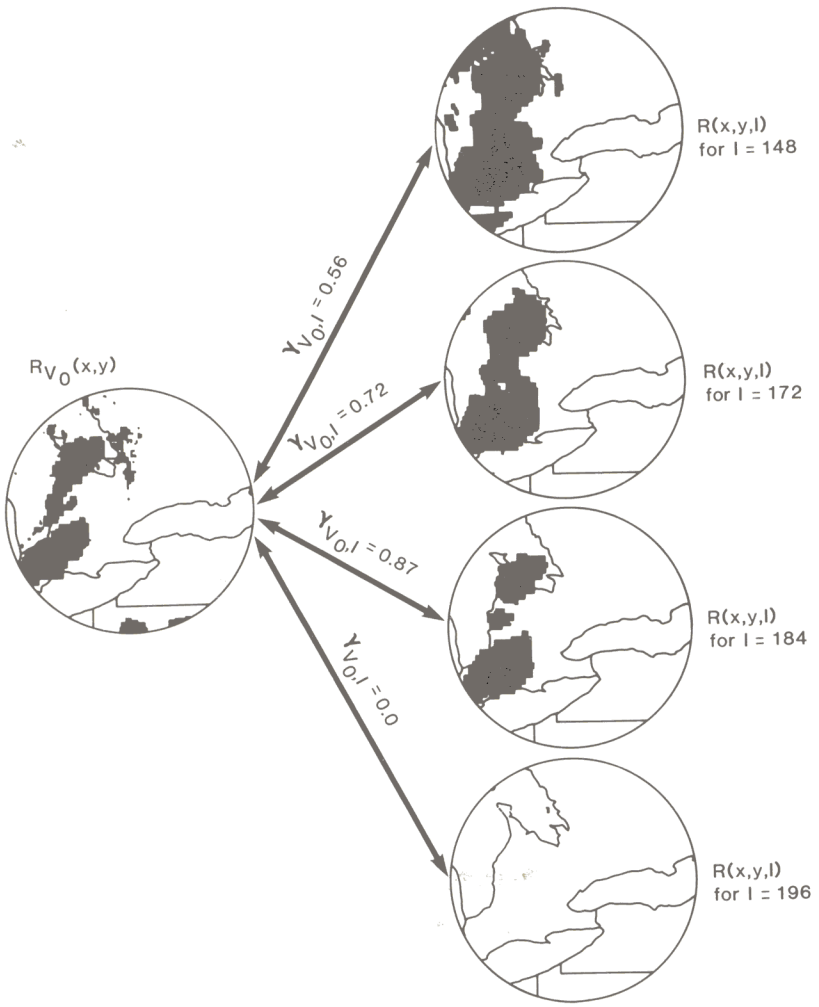

FIGURE 1. Cross-correlation ($\gamma_{V_0,I}$) between rain area as delineated by the Tsonis–Isaac technique [$R_{V_0}(x, y)$] and rain area as delineated by four different infrared thresholds [$R(x, y, I)$].

TABLE 1 Summary of the Satellite and Radar Data Used in This Study

	Date	Period (GMT)	Type of Precipitation
Training sample	2 May 1983	1730	C
	6 June 1983	1230–1730	N-C
	27 June 1983	1430–2200	N-C, C
	4 July 1983	1230–2330	C
	21 July 1983	1730–2300	C
	29 July 1983	1330–2330	N-C
Verifying sample	27 July 1982	1230–1900	N-C
	28 July 1982	1400–2200	C
	3 Aug. 1982	1200–2300	N-C
	13 May 1984	1330–1900	N-C
	23 May 1984	1300–2200	N-C, C

images is 8×8 km. From these images 4×4 km resolution images have been constructed for a better resolution equivalence between the infrared and visible data. The count range of the visible image is 0–63 and that of the infrared is 0–255.

The analysis of the data was restricted to the area in Ontario, Canada, which is covered by the C-band Woodbridge weather radar. Table 1 gives a summary of the satellite and radar data used in this study. The radar data was used mainly for verification purposes. The third column indicates the type of precipitation (C for convective and N-C for nonconvective). For more details on the data, see Tsonis (1984) or Tsonis and Isaac (1985).

Method and Data Analysis

This work is based on the method and results of instantaneous rain area delineation in the midlatitudes from GOES imagery reported in Tsonis and Isaac (1985). Their method is composed of two parts: a technique for the discrimination between raining and nonraining clouds and a scheme for the delineation of the rain area. Although some restrictions apply, the delineation of the rain area from the raining clouds is based on an optimum visible threshold (V_0) which varies according to the day, time, and type of precipitation. Hereafter, any rain area determined by the Tsonis–Isaac method will be denoted as $R_{V_0}(x, y)$. The reported average accuracy in estimating $R_{V_0}(x, y)$ considering convective and nonconvective cases is about 70% (the accuracy increases if only convective cases are considered).

The Tsonis–Isaac (1985) method is oriented toward instantaneous rain area delineation using only visible and infrared images and does not require radar data or life-history knowledge. The main conclusion of the Tsonis and Isaac (1985) work was that the visible images contain more information about the areal extent of precipitation in the midlatitudes than the infrared images, except in cases of strong convection. In such cases, some optimum infrared threshold (I_0) can be as effective as V_0. In nonconvective or weak convection cases, any infrared threshold fails to delineate the rain area satisfactorily but the visible threshold (V_0) does not (for more details, see Tsonis and Isaac, 1985).

These earlier findings will be examined here for the purpose of inferring more information about $R_{V_0}(x, y)$. Following the Tsonis–Isaac (1985) method for rain area delineation in the midlatitudes, the approach taken here is oriented toward extracting information about the intensity and type of the precipitation using only the satellite data. It will be assumed that $R_{V_0}(x, y)$ is a good estimation of the actual rain area. Radar data will be used only for verification purposes. The method to be employed involves the concept of the degree of matching between two two-dimensional patterns $P_1(x, y)$ and $P_2(x, y)$. The degree of matching between any two rain area patterns, $P_1(x, y)$ and $P_2(x, y)$, can be determined by their cross-correlation which is expressed mathematically as follows:

$$\gamma = \frac{1}{NS_1S_2} \iint [P_1(x, y) - \bar{P}_1] \times [P_2(x, y) - \bar{P}_2]\, dx\, dy, \qquad (1)$$

where:

a. γ is the cross-correlation between $P_1(x, y)$ and $P_2(x, y)$ $(0 \leqslant \gamma \leqslant 1)$.
b. $N = \iint dx\, dy$ is the area of integration which must contain both patterns.

c. $P_1(x, y)$ and $P_2(x, y)$ are the spatial distributions of the patterns under consideration.

d. $\bar{P}_1, \bar{P}_2$ are the average values of the fields $P_1(x, y)$ and $P_2(x, y)$ over the area N, i.e.,

$$\bar{P}_1 = \iint P_1(x, y)\, dxdy/N.$$

e. S_1, S_2 are the standard deviations of $P_1(x, y)$ and $P_2(x, y)$ over N, i.e.,

$$S_1 = \left[\iint [P_1(x, y) - \bar{P}_1]^2\, dxdy/N\right]^{1/2}.$$

Let us now assume that a scheme is devised which simply delineates the rain area using a single infrared threshold (I). Given an infrared image, starting with some low threshold, one can produce a series of smaller rain areas by raising stepwise an infrared threshold. By raising the threshold value (I), the resulting rain area will become smaller and smaller. Let us denote these areas as $R(x, y, I)$.

Based on the foregoing assumptions, in cases of strong convection, there will exist some $I = I_0$, for which $R(x, y, I_0) \approx R_{V_0}(x, y)$. Under this condition, for $P_1 = R_{V_0}(x, y)$ and $P_2 = R(x, y, I_0)$, γ should be high. In addition, for $I > I_0 \Rightarrow R(x, y, I) < R(x, y, I_0)$ and for $I < I_0 \Rightarrow R(x, y, I) > R(x, y, I_0)$. Therefore, it follows that for $I \neq I_0$ the cross-correlation between $R(x, y, I)$ (for any I) and $R_{V_0}(x, y)$ will be lower than the cross-correlation between $R(x, y, I_0)$ and $R_{V_0}(x, y)$. If we denote as $\gamma_{V_0, I}$ the cross-correlation between $R_{V_0}(x, y)$ and $R(x, y, I)$, it should be expected that $\gamma_{V_0, I}$ as a function of (I) would reach a maximum for $I = I_0$. The above can be visualized in Fig. 1. On the left side of Fig. 1, $R_{V_0}(x, y)$ indicates the rain area delineated by the optimum visible threshold according to the Tsonis–Isaac (1985) method. Satellite information for 1730 GMT, 2 May 1983 was used. The radar data indicates moderate to heavy convective precipitation at this time. On the right side of Fig. 1, rain areas determined by four different infrared thresholds are shown. The cross-correlation between $R_{V_0}(x, y)$ and each of $R(x, y, I)$ is also shown. As can be seen in Fig. 1, $R(x, y, I)$ decreases in size as (I) increases, whereas the degree of matching between $R(x, y, I)$ and $R_{V_0}(x, y)$ [from Eq. (1)] increases attaining a maximum value for $I = I_0 \approx 184$. In nonconvective cases, $R(x, y, I)$ (for any I) may deviate significantly from $R_{V_0}(x, y)$ and therefore $\gamma_{V_0, I}$ may neither be as high nor vary as a function of (I) in a similar fashion.

Therefore, the evaluation of $\gamma_{V_0, I}$ may be beneficial in inferring rainfall rates or in discriminating between convective and nonconvective precipitation.

Figure 2 shows $\gamma_{V_0, I}$ as a function of (I) for nine selected cases from the training sample which represent convective and nonconvective cases of various rainfall intensities. The classification into light, moderate, and heavy rainfall corresponds to the radar rainfall rate intervals $0 \leqslant R \leqslant 2$ mm h^{-1}, $2 < R \leqslant 8$ mm h^{-1}, and $R > 8$ mm h^{-1}, respectively. The infrared threshold was varied from 148 (-17°C) to 208 (-63°C). First, let us concentrate on the cases of 2 May 1983 at 1730 GMT and 4 July 1983 at 2230 GMT, which represent convective cases (as indicated by the radar) of moderate to heavy rainfall. In both cases, $\gamma_{V_0, I}$ in-

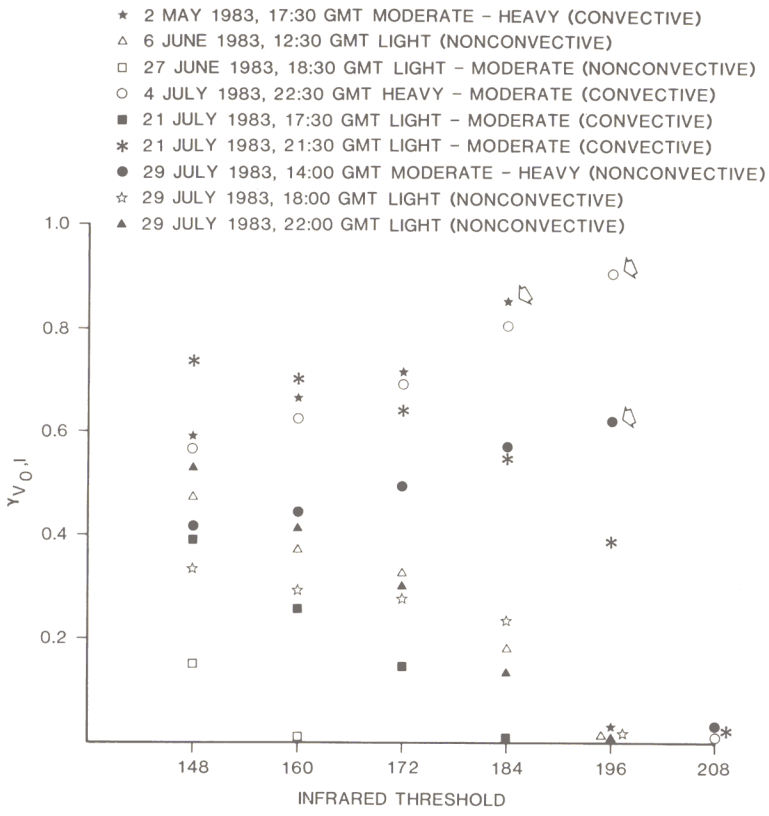

FIGURE 2. $\gamma_{V_0,I}$ as a function of the infrared threshold for various precipitation types and intensities: (★) 2 May 1983, 17:30 GMT moderate–heavy (convective); (△) 6 June 1983, 12:30 GMT light (nonconvective); (□) 27 June 1983, 18:30 GMT light–moderate (nonconvective); (○) 4 July 1983, 22:30 GMT heavy–moderate (convective); (■) 21 July 1983, 17:30 GMT light–moderate (convective); (✱) 21 July 1983, 21:30 GMT light–moderate (convective); (●) 29 July 1983, 14:00 GMT moderate–heavy (nonconvective); (☆) 29 July 1983, 18:00 GMT light (nonconvective); (▲) 29 July 1983, 22:00 GMT light (nonconvective).

creases as (I) increases and attains maximum value (pointed by arrows) for $I = 184$ and $I = 196$, respectively. The cross-correlation then decreases for higher I's [i.e., $R(x, y, I) \to 0$]. Note that the observed maximum value of the cross-correlation is very high in both cases. A similar pattern can be observed in the 29 July 1983, 1400 GMT case. This case represents a nonconvective rain area of predominantly moderate precipitation. Here again, $\gamma_{V_0,I}$ increases as (I) increases and attains a maximum value for $I = 196$. However, the magnitude of the maximum cross-correlation in this case is not as high as in the convective case. In all other cases, which represent either cases of weak convection or nonconvective cases, $\gamma_{V_0,I}$ decreases constantly as (I) increases (that is, the maximum correlation occurs at thresholds around or lower than 148).

From the available training data set, 27 different cases were studied. Fourteen of those cases were convective cases; seven were associated withmoderate to heavy rainfall, and seven were associated with

light to moderate rainfall. The remaining cases were nonconvective. Six were associated with predominantly moderate rainfall, four were associated with light to moderate rainfall, and three were associated with just light rainfall. Although the temporal resolution of the data is 30 min, only cases that were at least 1.5 h apart were included in the sample. This restriction limits the size of the sample to be studied but minimizes the degree of dependency in the sample. In all cases of moderate to heavy rainfall (whether convective or not), $\gamma_{v_0, I}$ increased with (I) and attained a maximum value for some (I) which was always greater than 170. However, the magnitude of this maximum cross-correlation was, on the average, higher for the convective cases, where it was found to range between 0.68 and 0.92 (mean value equal to 0.83). The corresponding range for the nonconvective cases was 0.52–0.72 (mean value equal to 0.62). For all cases of light to moderate rainfall (whether convective or not) the best matching occurred at infrared thresholds lower than 150. Figure 3 gives the location (with respect to the infrared threshold) and magnitude of the maximum $\gamma_{v_0, I}$ for the 27 cases studied. Apparently, the location and magnitude of the maximum $\gamma_{v_0, I}$ can provide some information about the type and intensity of $R_{v_0}(x, y)$. In view of the discussion above, these findings come as no surprise and indicate that the infrared images are not as effective as the visible images for rain area delineation in the midlatitudes in cases of weak or no convection. The cross-correlation procedure may be thought of as a "tuning" procedure similar to the procedure of tuning a radio set

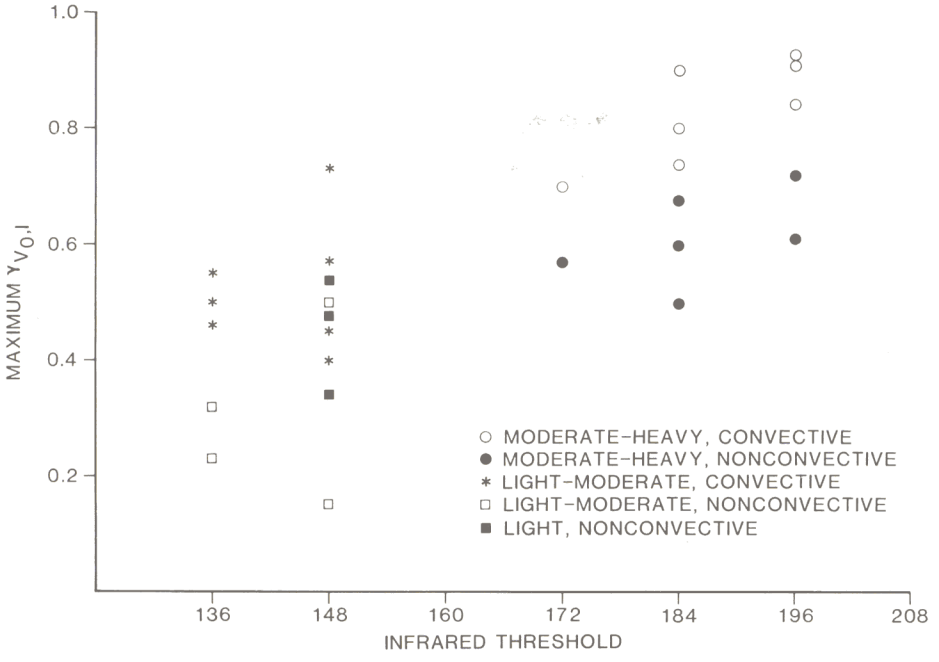

FIGURE 3. Magnitude and location (with respect to the infrared domain) of the maximum $\gamma_{v_0, I}$ for each one of the 27 cases that were included in the training sample: (○) moderate–heavy, convective; (●) moderate–heavy, nonconvective; (*) light–moderate, convective; (□) light–moderate, nonconvective; (■) light, nonconvective.

where a trial frequency $[R(x, y, I)$, for any $I]$ is compared to an incoming frequency $[R_{V_0}(x, y)]$. If the frequencies coincide, then a signal of high power is obtained (high correlation). If not, a weak signal is obtained.

Verification

The above findings were then incorporated into a simple scheme which was applied to 25 cases from the verifying data set. For each of these cases, $R_{V_0}(x, y)$ was again determined by the Tsonis–Isaac method and $\gamma_{V_0, I}$ was computed as a function of the infrared threshold (I). If the maximum $\gamma_{V_0, I}$ was observed at an $I \geqslant 160$, then the delineated rain area was classified as moderate to heavy. If at the same time the magnitude of the maximum $\gamma_{V_0, I}$ was $\geqslant 0.70$, then the rain area was characterized as convective. On the other hand, if the magnitude of the maximum was < 0.70, then the rain area was characterized as nonconvective. In all other cases the delineated rain area is classified as light to moderate, and no characterization as convective or nonconvective is attempted. The classifications were then compared to what was actually observed and the results were summarized in Table 2. The entries in Table 2 indicate how many times a given situation was classified correctly or incorrectly. For example, six out of seven moderate to heavy convective events were classified correctly. In Table 2 the sum of the entries in the diagonal would give the total number of cases correctly classified. Therefore, the overall accuracy of the scheme is 84% (21/25). It should be noted that most of the classification error results from errors in characterizing the type of the precipitation. The discrimination between light to moderate and moderate to heavy events is very successful.

Conclusions

This study made use of the Tsonis–Isaac (1985) technique for rain area delineation in the midlatitudes with the use of GOES data.

Although the distribution of intensity inside a rain area cannot be determined, results indicate that it is possible to classify the rain area as convective or nonconvective. Further, rain areas them-

TABLE 2 Verification Results from the Verifying Data Set

	Predicted			
	Moderate to Heavy		Light to Moderate Either Convective or Nonconvective	
Actual	Convective	Nonconvective		
Moderate to Heavy				
Convective	6	1	—	7
Nonconvective	2	6	—	8
Light to Moderate Either convective or nonconvective	—	1	9	10
	8	8	9	25

selves can be separated into two rainrate classes: light–moderate and moderate–heavy.

It was found that, if the maximum cross-correlation between the rain area as delineated by the Tsonis–Isaac technique and the rain area delineated by the infrared threshold count was greater (less) than 0.70, then the rain area was characterized as convective (nonconvective). Further, if the maximum cross-correlation was observed at an infrared count greater or equal to 160, then the delineated rain area was classified as moderate to heavy.

These encouraging results suggest that additional samples should be collected and analyzed in order to further test the procedure and the threshold values.

I would like to thank the Atmospheric Environment Service of Canada for providing me with the data and facilities for some of the data processing. I would also like to thank Ms. M. Kleiber for typing the manuscript and Mrs. Donna Schenstrom for drafting the figures.

References

Barrett, E. C., and Martin, D. W. (1981), *The Use of Satellite Data in Rainfall Monitoring*, Academic, New York, 340 pp.

Griffith, C. G., Woodley, W. L., Grube, P. G., Martin, D. W., Stout, J., and Sikdar, D. N. (1978), Rain estimation from geosynchronous satellite imagery—visible and infrared studies, *Mon. Weather Rev.* 106:1153–1171.

Lovejoy, S., and Austin, G. L. (1979), The delineation of rain areas from visible and IR satellite data for GATE and midlatitudes, *Atmos.-Ocean* 17:77–92.

Scofield, R. A., and Oliver, V. J. (1977), A scheme for estimating convective rainfall from satellite imagery, NOAA Tech. Memo. NESS 816, 47 pp.

Stout, J. E., Martin, D. W., and Sikdar, D. N. (1979), Estimating GATE rainfall with Geosynchronous Satellite Images, *Mon. Weather Rev.* 107:585–598.

Tsonis, A. A. (1984), On the separability of various classes from the GOES visible and infrared data, *J. Climate Appl. Meteorol.* 23:1393–1410.

Tsonis, A. A., and Isaac, G. A. (1985), On a new approach for instantaneous rain area delineation in the midlatitudes using GOES data, *J. Climate Appl. Meteorol.* 24:1208–1218.

Wu, R., Weinman, J. A., and Chin, R. T. (1985), Determination of rainfall rates from GOES satellite images by a pattern recognition technique, *J. Atmos. Oceanic Technol.* 2:314–330.

Received 10 March 1986; revised 15 July 1986.